Journal of Alloys and Compounds 509 (2011) 384–386

Contents lists available at ScienceDirect

Journal of Alloys and Compounds

journal homepage: www.elsevier.com/locate/jallcom

The effect of NH_3 concentrations on the electrical properties of N-doped ZnO and study on mechanism

Tang Li-dan[a,*], Wang Bing[a], Zhang Yue[b]

[a] Department of Materials Physics, Liaoning University of Technology, Jinzhou 121001, China
[b] Department of Materials Physics, Beijing University of Science and Technology, Beijing 100083, China

ARTICLE INFO

Article history:
Received 26 June 2010
Received in revised form 3 September 2010
Accepted 4 September 2010
Available online 16 September 2010

Keywords:
Thin films
Sputtering
Electrical properties

ABSTRACT

The N-doped ZnO films deposited by RF magnetron sputtering were treated under various NH_3 concentrations. The N-doped ZnO films were characterized by XRD, FESEM, Hall measurement and XPS. The XRD and SEM results showed that ZnO films were crystallized in the wurzite phase with a preferential orientation along the c axis and the surfaces were smooth and dense over the film. The Hall and XPS measurement indicated that N element had doped into ZnO crystal lattice, which is benefit for fabrication of p type ZnO films.

1. Introduction

ZnO with a direct band gap of 3.37 eV and large exciton binding energy of 60 meV has been receiving considerable attention due to the potential application as optoelectronic devices [1–3]. However, an important issue is the preparing of high quality p-type ZnO films. It has been proven difficult due to the self-compensation effect, deep acceptor level and low solubility of the acceptor dopant [4–6]. In recent years considerable efforts have been made to realize p-type ZnO by doping method. It is well known that nitrogen is the most promising candidate duo to small ionic size and low energy level of substitution (No) [7,8]. In this study we report the growth of N-doped ZnO films by radio frequency magnetron sputtering and post-annealing using NH_3 as a doping source. Effects of NH_3 concentrations on the structural and electrical properties of ZnO films will be discussed. Furthermore the N-doping mechanism is studied in detail.

2. Experimental procedures

N-doped ZnO films were deposited on quartz substrate by radio frequency magnetron sputtering and post-annealing method using NH_3 as a doping source. The quartz substrates were ultrasonically cleaned in acetone and in alcohol, respectively, and then rinsed in deionized water, subsequently dried in flowing nitrogen gas before deposition. During deposition the chamber was evacuated to a base pressure 5×10^{-4} Pa, and argon was introduced as the working gas with a pressure of 0.5 Pa. The ZnO films were grown with the thickness of ~360 nm measured by means of quartz vibrate frequency. The ZnO films were heated to 700 °C with flowing dry NH_3 atmosphere in a tube furnace. The NH_3 gas flow rate were 10 sccm (Sample A), 30 sccm (Sample B), 50 sccm (Sample C) and 70 sccm (Sample D), respectively. The temperature of the tube was held constant for 1 h to form N-doped ZnO films. Subsequently the Ni/Pt electrodes were deposited on ZnO films by using direct current magnetron sputtering of Ni target (99.999% purity) and Pt target (99.95% purity) to form perfect ohmic contact for electric measurement.

The crystalline structure of obtained ZnO films was analyzed by X-ray diffraction (XRD) (D/MAX-RB, Cu Kα). The morphology of the films was characterized by using field emission scanning electron microscopy (FESEM) (LEO-145, voltage 200–300 V, resolution 3–5 nm). The electrical properties were obtained by the four-probe van der Pauw method using Hall-effect measurement system (HL5500PC). X-ray photoelectron spectroscopy (XPS) was used to determine components with a spectrometer RIBER 200 surface analysis system.

3. Result and discussion

Fig. 1(a) shows XRD pattern of ZnO films treated under various NH_3 concentrations. In these XRD patterns only one peak is observed at 34–35°, which corresponds to the ZnO (0 0 2) diffraction, and no other peaks are detected. The XRD analysis indicates that all films are crystallized in the wurzite phase and present a preferential orientation along the c-axis. Fig. 1(b) shows corresponding shifts of the (0 0 2) peak position at various NH_3 concentrations. The intensity of (0 0 2) peaks change with NH_3 concentrations. It can be inferred that ZnO films annealed at the NH_3 gas flow rate of 30–50 sccm possess the best crystallinity. These (0 0 2) peaks position of N-doped ZnO films shift to small degree as NH_3 concentrations increase because more N element have incorporated into ZnO crystal lattice with NH_3 concentrations increasing.

* Corresponding author. Tel.: +86 0416 4199650.
E-mail address: kittytld@yahoo.com.cn (T. Li-dan).

0925-8388/$ – see front matter © 2010 Elsevier B.V. All rights reserved.
doi:10.1016/j.jallcom.2010.09.032

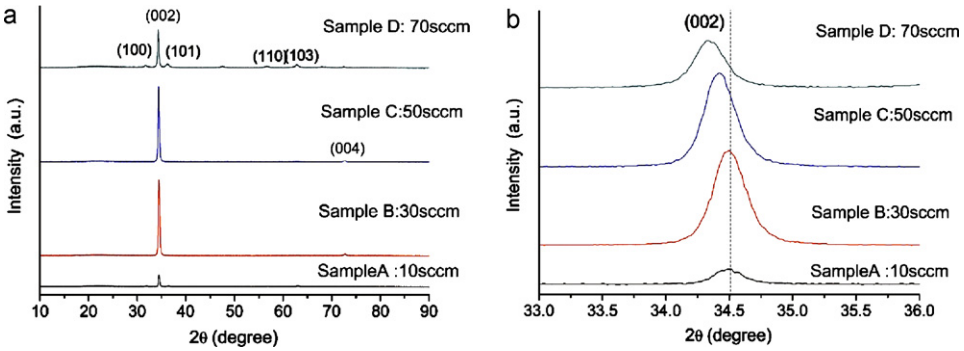

Fig. 1. (a) XRD pattern of ZnO films treated under various NH_3 concentrations and (b) corresponding shifts of the (0 0 2) peak position at various NH_3 concentrations.

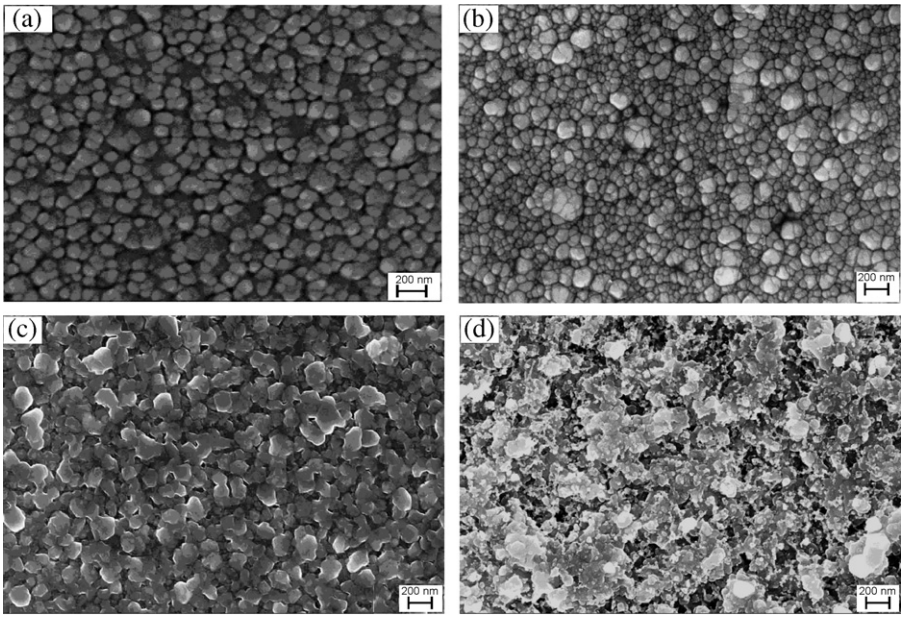

Fig. 2. SEM photomicrographs of ZnO films treated under various NH_3 concentration. (a) 10 sccm; (b) 30 sccm; (c) 50 sccm; (d) 70 sccm.

Fig. 2 presents SEM photomicrographs of ZnO films treated under various NH_3 concentrations. The SEM images show that these films have uniform thickness, smooth surface without visible pores and defects, as indicated in Fig. 2(a)–(c). When NH_3 gas flow rate increases to 70 sccm ZnO film surface with many visible pores is not compact as showed in Fig. 2(d). This is mainly duo to ammonia corrosive characteristics. The reaction equations are below [9]:

$$NH_3 \rightarrow NH^{2-} + 2H^+ \quad (1)$$

$$ZnO + 2H \rightarrow Zn + H_2O \quad (2)$$

The electrical properties of ZnO films annealed under various NH_3 concentrations are measured in Table 1. It is obvious that electrical properties of ZnO films are dependent on the NH_3 concentrations. With NH_3 concentrations increasing the resistivity of ZnO films increase because more N element had doped into ZnO crystal lattice to form acceptor dopant. In addition Table 1 shows that p-type conductivity of both Sample B and Sample C are weak and the Hall mobility of Sample B was only 0.015 cm^2/V. Such low mobilities may be due to high interface defect densities [10]. When the ammonia concentration is too high (Sample D) the resistivity of Sample D is too big to measure the conduct type of films, which is probably relate to the fact that higher ammonia concentrations may arouse the dissociation of ZnO and destroy dense structure of ZnO films.

In order to gain a deeper insight into the N-doping mechanism, components of ZnO films are measured by XPS and these results are shown in Fig. 3. Fig. 3(a) shows a typical XPS wide scan spectrum. All the peaks had been indexed in the figure. Zn and O peaks are observed such as $Zn2p_{3/2}$, $Zn2p_{1/2}$, O_{1s} and so on, but the N peaks are not seen in XPS survey spectrums. Fig. 3(b) indicates that binding energies of $Zn2p_{3/2}$ and $Zn2p_{1/2}$ peaks are 1022.3 eV and 1045.3 eV, respectively, basically identical with Zn^{2+}. Compared with standard

Table 1
Electrical properties of ZnO films annealed under various NH_3 concentrations.

Sample	NH_3 gas flow rate (sccm)	Resistivity (Ω cm)	Hall mobility (cm^2/V)	Carrier concentration (cm^{-3})	Conduction type
A	10	1.165	1.178	1.690×10^{18}	n
B	30	25.014	0.015	8.346×10^{18}	P
C	50	30.257	0.011	9.207×10^{18}	P
D	70	2147	–	–	–

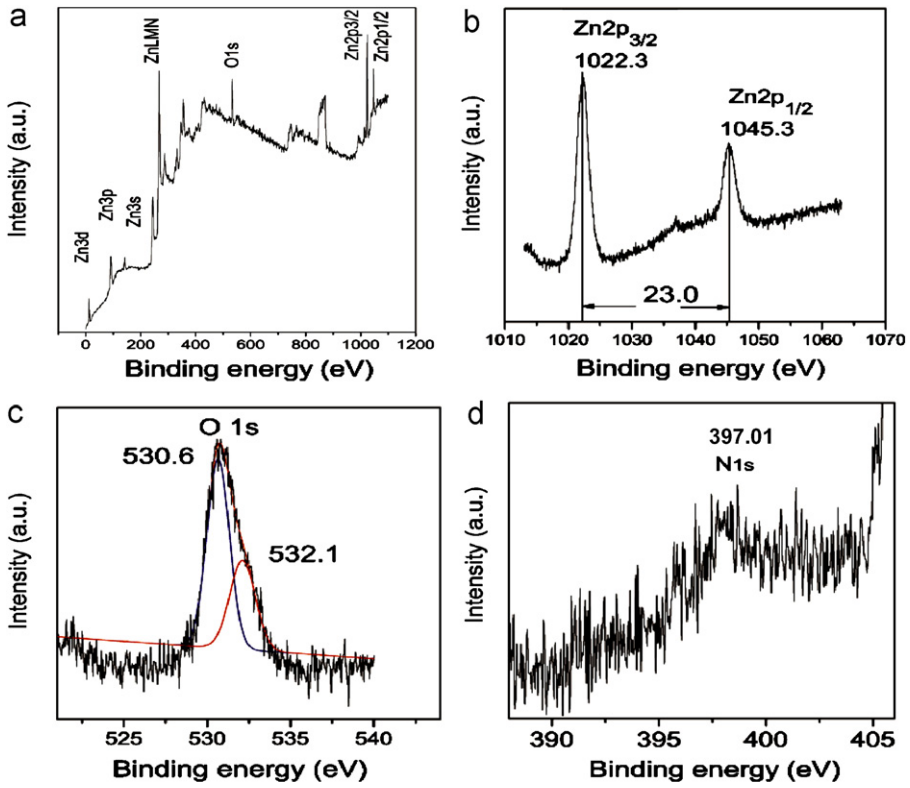

Fig. 3. XPS pattern of ZnO films. (a) XPS wide scan spectrum of ZnO, (b) Zn region, (c) O region, and (d) N region.

spectrum binding energies of $Zn2p_{3/2}$ and $Zn2p_{1/2}$ peaks shift to high energy, which indicated no metal zinc exist in ZnO films [11]. Fig. 3(c) presents the O_{1s} peak of ZnO film. The O_{1s} peak treated by Gauss had been divided into two peaks located at 530.6 eV and 532.1 eV. The peak (530.6 eV) is O_{1s} binding energy corresponding to Zn–O bond. The other peak (532.1 eV) comes from the surface adsorption of CO_2, H_2O and O_2 from air [12]. Fig. 3(d) shows a small peak at binding energy of 397.01 eV corresponding to the N_{1s} peak. The N_{1s} peak presents the formation of N–Zn bonds, which shows nitrogen atom slipped into oxygen vacancy as part of oxygen substitute of ZnO [13–15]. The process of doping could be explained as follow [16]:

$$ZnO + xNH^{2-} \rightarrow ZnO_{1-x}N_x + xH_2O \quad (3)$$

A consequence of the O^{2-} ion being replaced by N^{3+} introduces an acceptor level into the crystal. However N-doped ZnO film exhibited weak p-type conductivity due to native defects [17] and high interface defect densities [10]. In a word, N element had doped into ZnO crystal lattice to form acceptor doping, which is benefit for the apparent p type conductivity.

4. Conclusion

N-doped ZnO film deposited by magnetron sputtering at room temperature was fabricated successfully by annealing under ammonia atmosphere. And these N-doped ZnO films are crystallized in the wurzite phase with a preferential orientation along the c axis and the surfaces are smooth and dense over the film. The forming of p type conduction is due to nitrogen incorporation in ZnO films. Hall and XPS measurement results indicated that N element had doped into ZnO crystal lattice, which is benefit for fabrication of p type ZnO films.

Acknowledgment

The work was supported by National Basic Research Program of China (No. 2007CB936201).

References

[1] Ü. Özgür, Y.I. Alivov, C. Liu, A. Teke, M.A. Reshchikov, S. Doğan, et al., J. Appl. Phys. 98 (2005) 041301.
[2] Z.K. Tang, G.K.L. Wang, P. Yu, M. Kawasaki, A. Ohtomo, H. Koinuma, et al., Appl. Phys. Lett. 72 (1998) 3270–3272.
[3] D.C. Look, Mater. Sci. Eng. B 80 (2001) 383–387.
[4] B.J. Coppa, R.F. Davis, R.J. Nemanich, Appl. Phys. Lett. 82 (2003) 400–402.
[5] C.G. Van de Walle, Phys. Rev. Lett. 85 (2000) 1012–1015.
[6] F.K. Shan, G.X. Liu, W.J. Lee, B.C. Shin, J. Appl. Phys. 101 (2007) 053106.
[7] T. Atsushi, O. Akira, O. Takeyoshi, O. Makoto, M. Takayuki, S. Masatomo, et al., Nat. Mater. 4 (2005) 42–46.
[8] H. Matsui, H. Saeki, T. Kawai, H. Tabata, B. Mizobuchi, J. Appl. Phys. 95 (2004) 5882–5888.
[9] G.D. Yuan, Z.Z. Ye, Q. Qian, L.P. Zhu, J.Y. Huang, B.H. Zhao, J. Cryst. Growth 273 (2005) 451–457.
[10] H.L. Mosbacker, Y.M. Strzhemechny, B.D. White, P.E. Smith, D.C. Look, D.C. Reynolds, C.W. Litton, L.J. Brillson, Appl. Phys. Lett. 87 (2005) 012102.
[11] F. Masanobu, Y. Katsuaki, T. Osamu, Thin Solid Films 322 (1998) 274–281.
[12] H.T. Cao, Z.L. Peia, J. Gonga, C. Suna, R.F. Huanga, L.S. Wena, J. Solid State Chem. 177 (2004) 1480–1487.
[13] C.L. Perkins, S.H. Lee, X.N. Li, S.E. Asher, T.J. Coutts, J. Appl. Phys. 97 (2005) 034907.
[14] G.W. Cong, Appl. Phys. Lett. 88 (2006) 062110.
[15] J.P. Zhang, L.D. Zhang, L.Q. Zhu, Y. Zhang, M. Liu, X.J. Wang, et al., J. Appl. Phys. 102 (2007) 114903.
[16] H.Y. Wei, Y.S. Wu, L.L. Wu, C.X. Hu, Mater. Lett. 59 (2005) 271–275.
[17] M.D. McCluskey, S.J. Jokela, J. Appl. Phys. 106 (2009) 071101.